

Distinct Kinematic Properties of the Galactic Halo System as Revealed in the SDSS CEMP giant population

Jaehun Jeong¹, Young Sun Lee², Young Kwang Kim², Timothy C. Beers³, Jinmi Yoon³

¹Department of Astronomy, Space Science, and Geology, Chungnam National University, South Korea

²Department of Astronomy and Space Science, Chungnam National University, South Korea

³Department of Physics and JINA-CEE, University of Notre Dame, Notre Dame, IN 46556, USA



Abstract

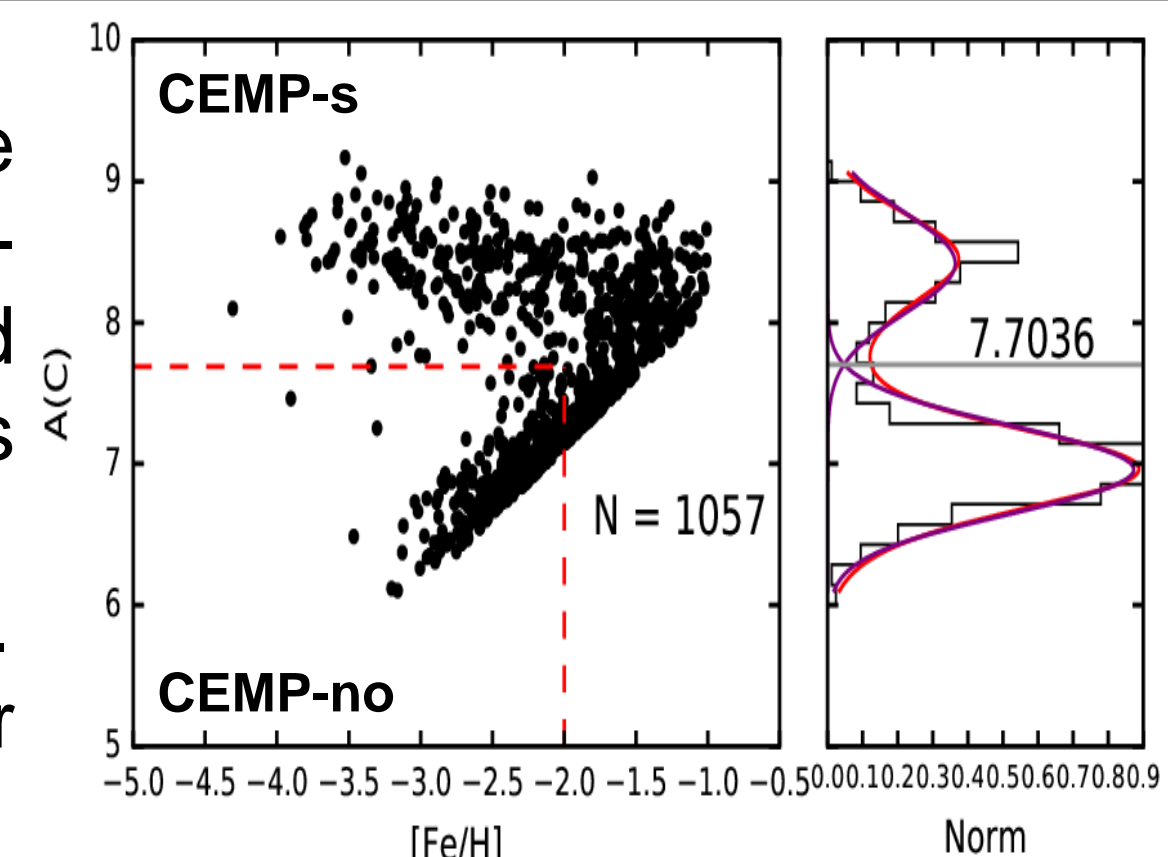
We report preliminary results on distinct chemical and kinematic features associated with the inner and outer halos of the Milky Way, as identified by metal-poor giants from the Sloan Digital Sky Survey (SDSS). In particular, using carbon-enhance metal-poor (CEMP) stars, we first map out the fractions of CEMP-no stars and CEMP-s stars in the inner- and outer-halo populations, separated by their spatial distribution of carbonicity ($[C/Fe]$). The CEMP-no and CEMP-s objects are classified by their different levels of absolute carbon abundances, $A(C)$. We investigate characteristics of rotational velocity and orbital eccentricity for these sub-classes within the halo populations. Distinct kinematic features for CEMP-no and CEMP-s stars identified in each halo region will provide important clues on the origin of the dichotomy of the Galactic halo.

Introduction

Our Milky Way halo system is expected to have gone through complicated formation and evolution processes, and is believed to have at least two distinct stellar populations as revealed from large spectroscopic data (Carollo et al. 2007, 2010). However, the existence of the duality and the origin of the Galactic halo are still on debate. To further investigate the dichotomy of the Galactic halo, we make use of carbon-enhanced-metal-poor (CEMP) stars observed by the Sloan Digital Sky Survey (SDSS). Among these objects, giants are powerful tracers to study the formation process of the Galactic halo system in situ. Selected giants in this study are in the range of $T_{\text{eff}} < 5600$ K and $\log g < 3.5$.

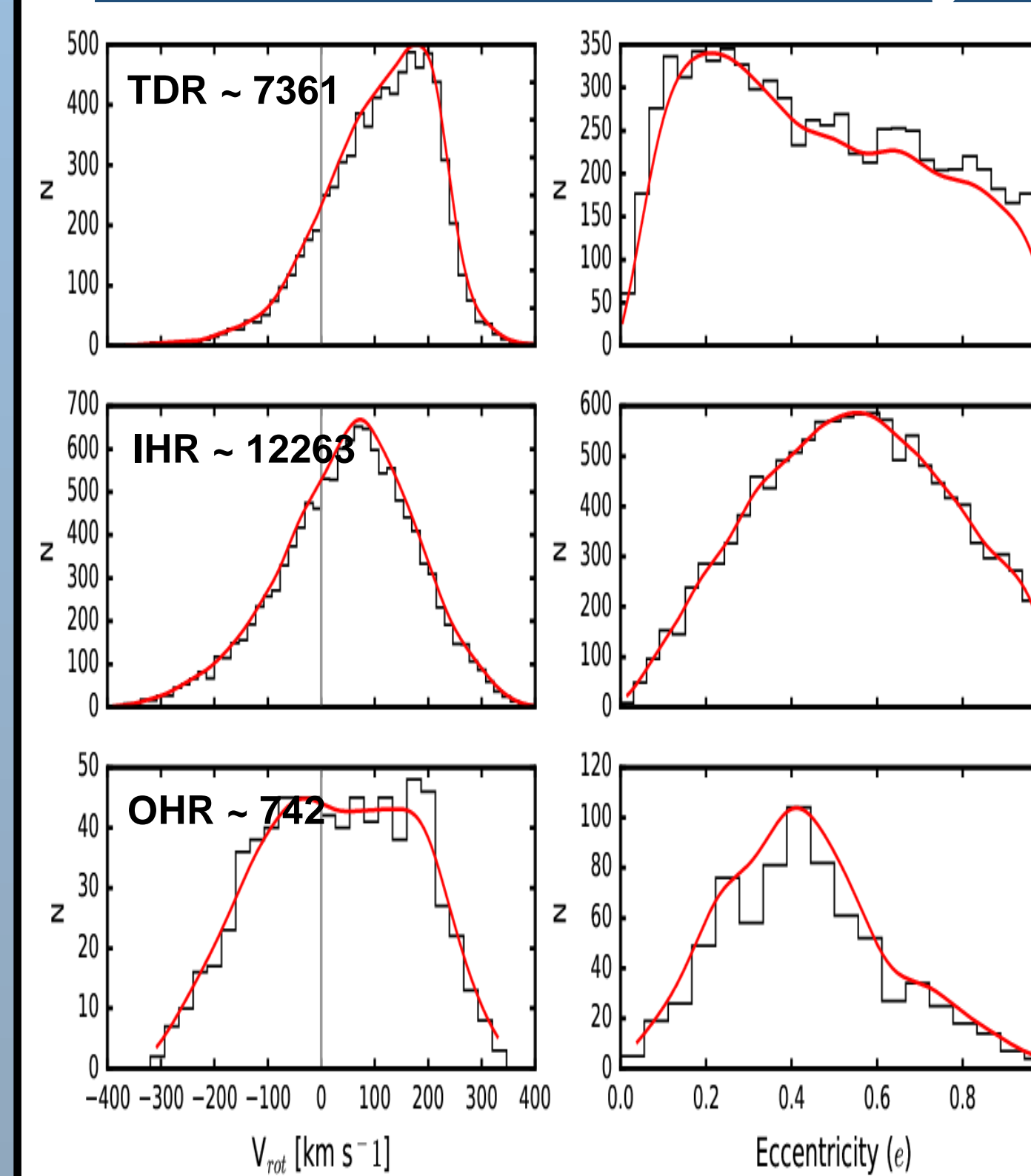
CEMP-no and CEMP-s Stars

- Using absolute carbon abundance ($A(C)$), we classified CEMP stars into CEMP-no (with no over-abundance of neutron capture elements) and CEMP-s (with over-abundance of s-process elements).
- We adopted Yoon et al. (2016) classification criteria.
- The right plot shows the classification method for our CEMP giants with $S/N > 30$.



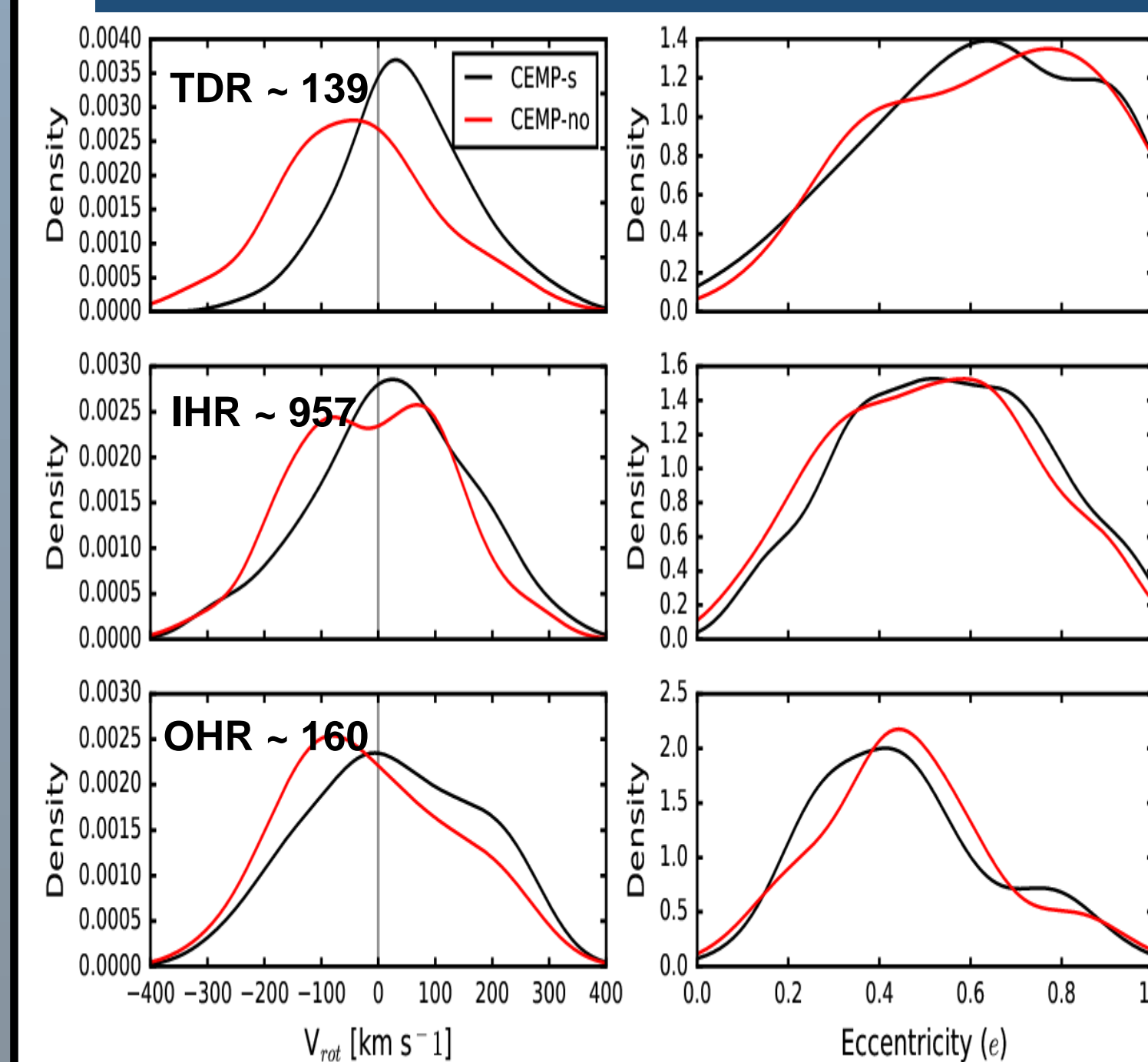
- The red dashed lines of the scatter plot separates the region of the CEMP-no stars from that of the CEMP-s stars. We adopted $A(C) \sim 7.7$ for the division of the two classes.

Rotation Velocity and Orbital Eccentricity



- The left panels show distributions of the rotation velocity (V_{rot}), while the right panels for the orbital eccentricity (e) in each Galactic region about all SDSS giant stars.
- The red curve is the Gaussian kernel density estimate.
- We notice that the OHR shows a larger portion of stars with retrograde motion with more low-eccentric stars, while the IHR exhibits the peak at slightly prograde motion with more eccentric orbit.
- These discrepancies in kinematics imply that the inner halo population has experienced different formation process from the outer halo population

Kinematics of CEMP-s and CEMP-no Stars



- Now we look at the rotation velocity and orbital eccentricity of CEMP-s and CEMP-no stars as shown in the left panels and right panels, respectively.
- The distributions are Gaussian kernel density estimates.
- There is more fraction of stars with retrograde motion among the CEMP-no stars in the IHR and OHR, while the eccentricity distribution does not look different between the CEMP-s and CEMP-no stars in each region.

Summary

- We used the SDSS CEMP giants to investigate the dichotomy of the Galactic halo.
- From the spatial distribution of $[C/Fe]$, we clearly evidenced the discontinuity around $|Z| \sim 19$ kpc, and could be divided into the IHR and OHR.
- In the IHR, we noticed smooth variation of $[C/Fe]$ with very small scatter, while the OHR shows large scatter with large error bars. This indicates that the IHR formed through dissipative collapse of proto-galactic clouds, which experienced continuous star formation in well-mixed gas environment, while the OHR possibly consists of many stars accreted from small fragments such as ultra faint dwarf galaxies, which experienced truncated star formation.
- This view is supported by the rotation velocity and eccentricity distribution of the CEMP giants in the IHR and OHR as we can expect that the accreted stars have more chances to be retrograde motion with circular orbit, while the dissipative collapsing gas could have chance to be prograde motion.

Reference

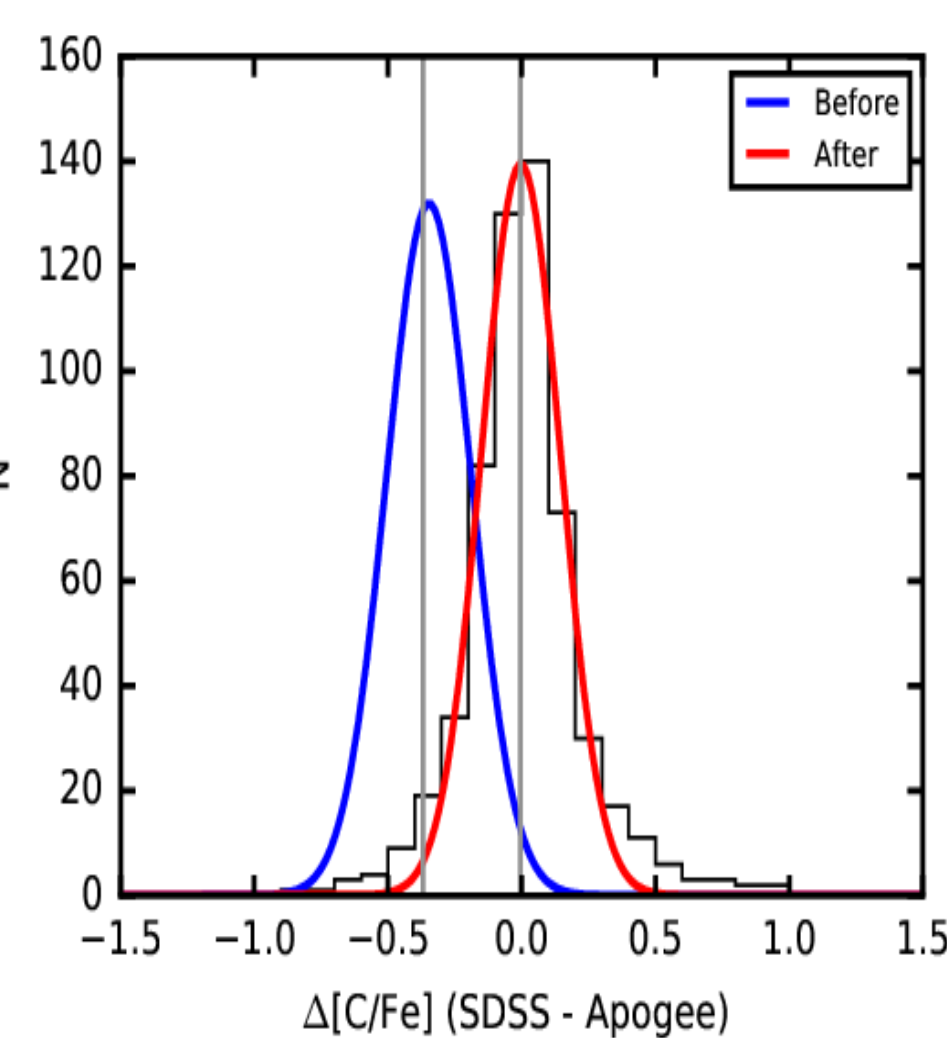
Carollo, D., et al. 2007, Nature, 450, 1020 Lee, Y. S., et al. 2017, ApJ, 836, 91
 Carollo, D., et al. 2010, ApJ, 712, 692 Placco, M. V., et al. 2014b, ApJ, 797, 21
 Chen, Y.Q., et al. 2017, ApJ, 795, 52 Yoon, J., et al. 2016, ApJ, 833, 20
 Lee, Y. S., et al. 2013, AJ, 146, 132

[C/Fe] Correction

- Because SDSS data are low-resolution ($R \sim 2000$) spectra, we first checked the accuracy and precision of our measured $[Fe/H]$ and $[C/Fe]$ (sometimes called "carbonicity") by comparing with overlapped stars from APOGEE DR14 data, which are based on high-resolution spectroscopy.
- We correct metallicity and carbonicity by:

$$[Fe/H]_{\text{corrected}} = [Fe/H]_{\text{SSPP}} + 0.125$$

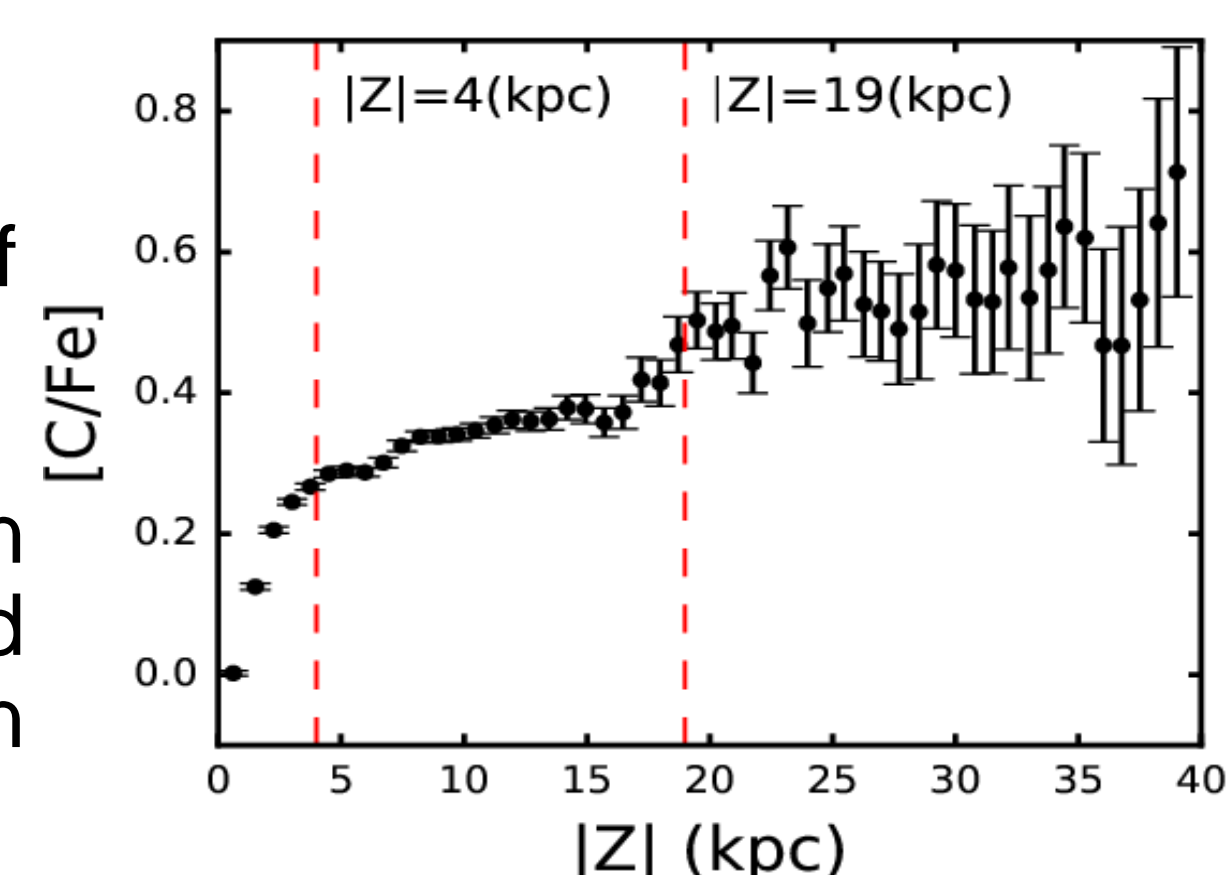
$$[C/Fe]_{\text{corrected}} = [C/Fe]_{\text{SSPP}} + 0.36$$



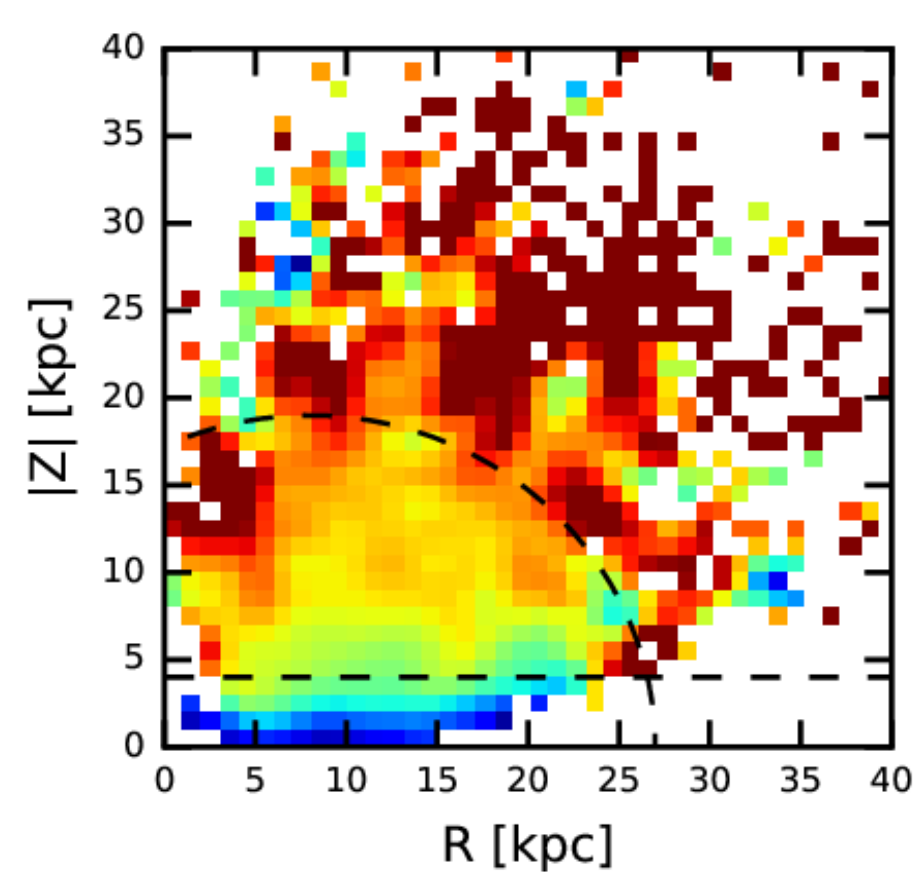
- A star that evolves along the red giant branch suffers from convection and extra mixing to dilute the carbon material, which causes measured $[C/Fe]$ lower than expected. This evolutionary effect is also corrected according to Placco et al. (2014) study.

Spatial Distribution of CEMP Giants

- We first looked at the spatial distribution of the CEMP giants as shown in the figures below, to check if there is any discontinuity in the level of $[C/Fe]$ as a function of $|Z|$ (absolute vertical distance from the Galactic plane).
- The right figure shows the mean carbonicity of all the giant stars in a bin of 1.5 kpc. Each bin is overlapped by 0.75 kpc with the next neighboring bin.
- We notice that the inner halo region (IHR) corresponds to $|Z| = 4 \sim 19$ kpc and $|Z| > 19$ kpc for the outer halo region (OHR).

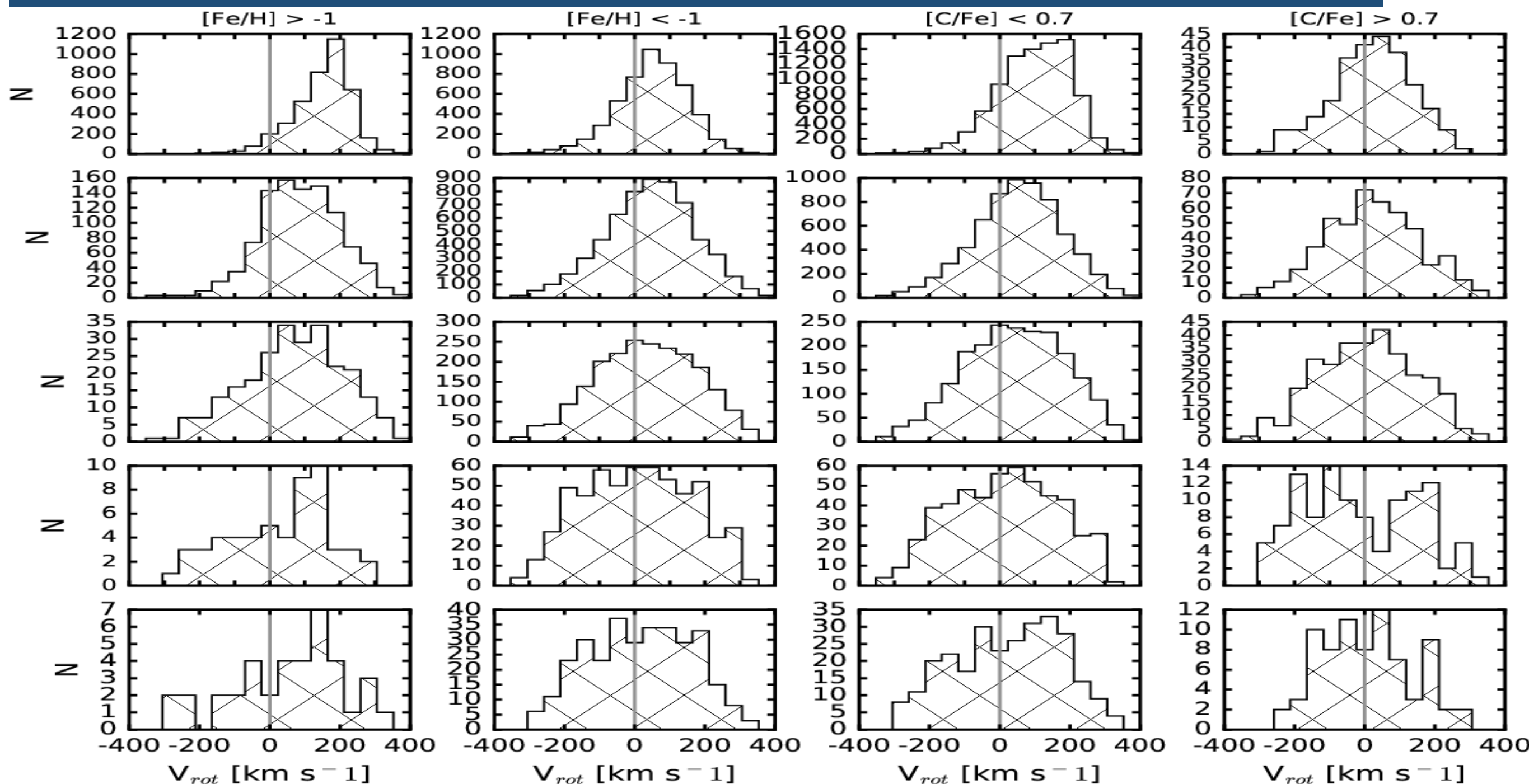


- In the figure above we note that the IHR shows very smooth variation of $[C/Fe]$ with very small error bars, while the OHR exhibits very large random distribution with large error bars. This behavior may arise from small number of stars in each bin, but it is more plausible to explain by accretion of stars with different level of carbon enhancement from various fragments such as ultra faint dwarf galaxies, suggesting the different origin of each halo region.



- The left figure shows the carbonicity map in the $|Z|$ and R plane.
- This map clearly shows the increasing trends of $[C/Fe]$ with increasing $|Z|$.
- The dashed curved line represents a heliocentric circle with a radius of 19kpc. This circle clearly delineates the different level of carbon enhancement in the map.

Distribution of Rotation Velocities



- The panels above indicate that at higher $|Z|$ distances, there are more fraction of regrade stars, especially for $[Fe/H] < -1.0$ or $[C/Fe] > 0.7$.